

X-RAY VARIABILITY OF ACTIVE GALACTIC NUCLEI: A UNIVERSAL POWER SPECTRUM WITH LUMINOSITY-DEPENDENT AMPLITUDE

A. LAWRENCE AND I. PAPADAKIS¹

Physics Department, Queen Mary and Westfield College, Mile End Road, London E1 4NS England
 Received 1993 January 27; accepted 1993 June 3

ABSTRACT

We present power-law model fits to the power spectra of 12 high-quality “long look” observations of AGNs from the *EXOSAT* data base. The AGNs concerned differ in X-ray luminosity L_x over a range 10^4 . The results are consistent with all objects having a power spectrum index equal to the mean value $\alpha = 1.55$. There is no correlation with L_x , suggesting that the power spectrum has little curvature over many decades of frequency. The mean slope is inconsistent with both standard shot-noise processes and traditional “ $1/f$ noise” but close to the prediction of simple “rotating hot spot” models. The power spectrum amplitude shows large object-to-object scatter but varies systematically as $L_x^{-0.5}$. This is inconsistent with any fixed-shape shot-noise model. Given the mean power spectrum slope, we then deduce that the time scale which gives fixed power spectral density varies as $\sim L_x^{0.3}$; however, the time scale below which there is fixed integrated power varies almost exactly linearly with luminosity.

Subject headings: galaxies: Seyfert — quasars: general — X-rays: galaxies

1. INTRODUCTION

The *EXOSAT* Observatory, with its capability of producing unbroken X-ray light curves up to 3 days long, transformed the study of the variability of active galactic nuclei (AGNs) from the “flare-spotting” phase to studies of the statistical character of variability. The basic result was that AGNs exhibit “red noise,” i.e., scale-free low-frequency divergent erratic variability (Lawrence et al. 1987; McHardy & Czerny 1987). There have since been discoveries of both a precise periodicity in NGC 6814 (Mittaz & Branduardi-Raymont 1989; Done et al. 1992) and intensity-dependent quasi-periodic oscillations in NGC 5548 (Papadakis & Lawrence 1993a). However, even in these cases variability is dominated by the red noise. Further progress obviously requires testing explicit models. The statistical behavior of power spectra is in principle well enough known to do this (see, e.g., van der Klis 1988), but standard techniques require heavy smoothing in order to make the error distribution of power spectrum estimates of known size and acceptably close to Gaussian; the smoothing also introduces large low-frequency bias. These problems have been removed with the new method of Papadakis & Lawrence (1993b), which results in spectral estimates that have 2–3 times better spectral resolution, that have exactly known variance, and which are exactly unbiased for power-law power spectra.

2. DATA SELECTION AND MODELING PROCEDURE

Light curves were extracted from the *EXOSAT* data base using bin sizes ranging from 50 to 300 s. Only the best observations were used, with stable background in the offset half of the medium energy (ME) instrument. Reliable results also require long observations, not only to ensure sufficient low-frequency “leverage” and a clear detection of variability above the Poisson noise of the light curve, but also because for short observations, the periodogram itself may be biased (see the Appendix in Papadakis & Lawrence 1993b). The zero-crossing time of the autocorrelation function of the object with strong-

est variability (NGC 4051) is $\sim 18,000$ s. We therefore took our minimum observation length, in order to avoid low-frequency bias, to be 70,000 s, i.e., 4 times this autocorrelation length. We used data from the ME only; data from the low energy (LE) imaging instruments mostly either had lower count rates or were interrupted by changes of filter. The result of selection was 12 observations of 11 AGNs, listed in Table 1. All extracted light curves and computed power spectra are shown in Papadakis (1993). The quantity “frms” is the fractional root mean square variation seen from the source (after subtracting Poisson noise). Notice that, because of the nature of red noise, this depends on observation length as well as source characteristics, so we cannot use this quantity directly to characterize the variability of a source, without first knowing the power spectrum slope.

The few gaps in the light curves were filled by linear interpolation plus appropriate Poisson noise. (Gaps constituted only a few percent of most time series and never more than 12%; gap-filling procedure makes little difference to our results.) Each light curve was divided by its mean value so that we work in fractional variability terms. The power spectrum was then estimated using the techniques of Papadakis & Lawrence (1993b). This involves averaging the logarithms of groups of periodogram values and taking these to be estimates of log spectral density at the geometric mean frequency of the periodogram points in the group. Based on simulations in Papadakis & Lawrence (1993b), we take groups of 20 periodogram points in order to get errors close to Gaussian, so that we can then proceed with standard χ^2 model fitting. In four cases (NGC 4593, Mrk 335, MR 2251, and NGC 5548), because the red noise was poorly constrained, we split the last bin into two groups of 10 periodogram points, to improve low-frequency leverage. To each power spectrum we fitted a power-law model:

$$\log [P(\nu)] = \log [A(10^4\nu)^{-\alpha} + C] . \quad (1)$$

Here A is the amplitude of the power spectrum at 10^{-4} Hz, and C is the constant component due to Poisson noise, which dominates at high frequency. This was not left free, but fixed at

¹ Current address: Physics Department, Southampton University, University Road, Southampton SO9 5NH England.

TABLE 1
OBSERVATION DETAILS AND MODEL FIT RESULTS

Name	Date ^a	Exposure (s)	frms	A (Hz ⁻¹)	α	χ^2_{\min}/dof	L_x (2–10 keV)
NGC 4051	1985/337	208,000	37%	98^{+28}_{-22}	$1.46^{+0.15}_{-0.14}$	60.8/49	41.70
NGC 6814	1985/289	102,000	19	35^{+7}_{-7}	$1.06^{+0.52}_{-0.13}$	15.4/15	42.51
NGC 4151	1983/192	86,700	14	$5^{+0.8}_{-0.8}$	$1.95^{+1.0}_{-0.4}$	10.0/19	43.00
NGC 4151	1986/060	82,700	7	$4^{+1.0}_{-0.6}$	$1.30^{+1.7}_{-0.3}$	12.1/18	42.83
MCG 6-30-15	1986/028	183,800	25	39^{+8}_{-8}	$1.48^{+0.19}_{-0.18}$	47.3/43	43.05
NGC 4593	1986/009	95,7000	16	27^{+3}_{-3}	$2.30^{+1.0}_{-0.46}$	3.6/10	43.10
Mrk 766	1985/363	193,800	29	71^{+32}_{-14}	$1.73^{+0.7}_{-0.4}$	10.7/14	43.34
NGC 5506	1986/024	225,600	12	10^{+3}_{-2}	$1.8^{+0.3}_{-0.2}$	56.1/54	43.38
Mrk 335	1985/202	74,100	18	33^{+7}_{-6}	$0.84^{+0.6}_{-0.2}$	10.1/11	43.58
NGC 5548	1986/062	85,900	11	8^{+6}_{-7}	$1.26^{+25.0}_{-0.60}$	30.3/20	43.81
				$6.3^{+0.7}_{-0.6}$	$1.96^{+0.98}_{-0.83}$	12.6/17	43.81 ^b
MR 2251	1983/279	91,800	10	$4.3^{+1.0}_{-1.0}$	$0.2^{+0.50}_{-0.004}$	12.1/9	44.80
3C 273	1986/017	145,200	4	$0.35^{+0.08}_{-0.07}$	$0.59^{+0.72}_{-0.50}$	39.4/34	46.10

^a Format: year/day of year.

^b Power-law component from fit with additional Gaussian component describing QPO, from Papadakis & Lawrence 1993a.

the value expected from the observed count rate. The errors shown are 68% confidence allowing other parameters to vary freely. Two sample power spectra, and their fitted models, are shown in Figure 1. Finally, we considered whether residual background variations may contribute to the variability seen, by taking the light curves of background halves, and estimating the Poisson-subtracted variance. This is negligible com-

pared to the observed source variances in almost all cases; the worst cases are MR 2251 and 3C 273, where we estimate that background variations could contribute up to $\sim 30\%$ of the observed variance.

3. MODEL FITTING RESULTS

The fitted amplitudes vary widely. The α values are generally between 1 and 2. This apparently differs significantly from the original claims of more or less exact “ $1/f$ ” noise for AGNs (Lawrence et al. 1987; McHardy & Czerny 1987), but those claims were based only on “eyeball fits” to heavily smoothed power spectra. We find the weighted mean value to be $\bar{\alpha} = 1.55 \pm 0.09$, and the data points are consistent with a constant value equal to this mean ($\chi^2 = 12.6$ with 11 data points). Most convincingly, the data sets that give the smallest errors all give values very close to $\alpha = 1.55$. Although we cannot rule out some spread, the data strongly suggest that this really is a universal value. The fits are acceptable at 90% confidence or better for all cases except NGC 5548. The latter exception is because of the broad QPO feature discussed in Papadakis & Lawrence (1993a). We have therefore used values of A and α from a model fit with an additional Gaussian component, as described in that paper. NGC 4151 was observed twice; for the correlations below, we averaged the fitted parameter values.

As a power law is an acceptable fit, we can say little about more complex continuum shapes. For example, as power is diverging to low frequencies, we must expect a knee somewhere; the present data only tell us that typically the knee time scale must be greater than $\sim 10^5$ s. By comparison with X-ray binaries, we might guess that in reality the power spectra are slowly curving between $\alpha = 1$ and $\alpha = 2$ over several decades of frequency (e.g., Belloni & Hasinger 1990a, b; Miyamoto, Kimura, & Kitamoto 1991). In this case, we are measuring an effective α over a limited frequency range. Although we can say no more about the gross continuum shape, this does not necessarily mean there are no significant *local* features. For example, by examining the residuals from best-fit parameters at higher resolution, we confirm the reality of the periodic signal in NGC 6814, as discussed by Mittaz & Branduardi-Raymont (1989), and Fiore, Massaro, & Barone (1992), at roughly 3% signifi-

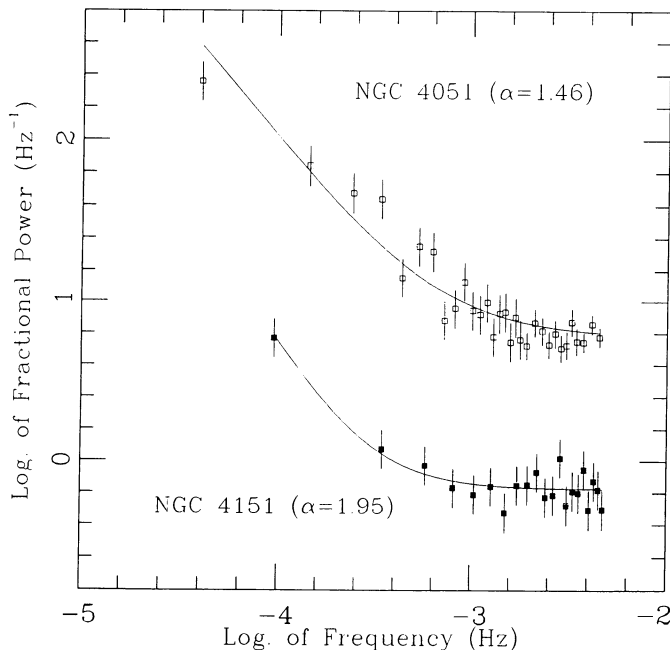


FIG. 1.—Power spectra of NGC 4051 and the first observation of NGC 4151, together with model fits as in Table 1. Individual points represent logarithmic averages of 20 periodogram points, except that for clarity of presentation, a larger binning has been used at the high-frequency end in the NGC 4051 plot. Errors bars are $\pm 1 \sigma$. Note that (1) NGC 4151 has a much higher count rate, and so has a lower Poisson level; (2) the NGC 4051 observation was longer, so extends to lower frequency; and (3) NGC 4051 has much stronger variability as well as a longer observation, and so is detected above the Poisson level over a larger frequency range; this means that the slope is well determined in NGC 4051, but poorly constrained in NGC 4151. In both cases the amplitude is well determined.

cance; however, this feature makes negligible difference to the global χ^2 .

4. CORRELATIONS WITH LUMINOSITY

It has been folklore for a long time that less luminous AGNs vary more rapidly. The first hard evidence of this was shown by Barr & Mushotzky (1986) who compiled the fastest known variation, Δt_{\min} , for a large sample of AGNs and showed this to correlate with X-ray luminosity. However, the statistical validity of the correlation has been questioned by Stephen et al. (1987), and the meaning and reliability of Δt_{\min} is most unclear, depending as much on observational history as on source characteristics. With the *EXOSAT* long looks we can objectively assess the correlation with *typical* variability. McHardy (1988) has argued that the *EXOSAT* data confirm the trend with luminosity, but no formal fitting was done. With our new model fits we can also look at the *form* of this correlation.

Figure 2 (*lower*) shows the power spectral slope α versus L_x . As well as being consistent overall with $\bar{\alpha} = 1.55$, a regression analysis shows that the slope is not significantly different from

zero. There is a marginal suggestion that the highest luminosity objects have flatter power spectra, but it is not significant; those objects have large errors. We might expect characteristic times to scale in some way with the luminosity of an AGN (see discussion below). If then there is a universal power spectrum, in different objects we would be sampling different scaled-frequency ranges of this spectrum; an intrinsically curved power spectrum should then show itself as a correlation of effective α with L_x . The observed lack of such a correlation suggests that there is very little curvature over several decades of frequency. A more definite statement would require a more specific model. For example, if time scale is simply proportional to luminosity, and the power spectrum is like that of Cyg X-1 (e.g., Belloni & Hasinger 1990a), we would expect a systematic drift from $\alpha = 1$ to $\alpha = 2$ over a factor of 10^4 in L_x . This is not consistent with the data.

Figure 2 (*middle*) shows the power spectrum amplitude. Here a clear anticorrelation with L_x is seen, but the object-to-object scatter is considerably larger than the measurement errors. We have fitted a straight line to $\log A$ versus $\log L_x$ using both simple regression and the “least-squares bisector line” method (Isobe et al. 1990). The result is almost identical: $A \propto L_x^{-\beta}$ with $\beta = 0.53 \pm 0.05$. (We have taken the true error on all points to be given by the average scatter about the fit. Below, we further assume that the real uncertainty on β is of the order 0.1.) Simple proportionality, $A \propto L_x^{-1}$, is ruled out at better than 95% confidence. We therefore confirm the qualitative claims of Barr & Mushotzky (1986) and McHardy (1988) but show that the effect is *not* one of simple proportionality.

It may be more useful to ask how some characteristic *time scale*, rather than a characteristic *amplitude*, varies with luminosity. Estimating such time scales necessarily involves extrapolating, and the individual α values are poorly determined. We therefore limit ourselves to calculating such time scales *on the assumption* that a universal $\alpha = 1.55$ applies. First, we ask at what frequency (and thus corresponding time scale) we get a fixed spectral power. This gives $T_1 \propto L^{0.34 \pm 0.07}$. However, a characteristic of red noise is that the longer one observes a source, the larger the rms spread of light curve values will be seen. One can then ask, how long an observation, T_2 , is needed in order to see a given rms variation? This involves all Fourier components from $\nu = 1/T_2$ upwards, and so we find that $T_2 \propto L^{1/(\alpha-1)} = L^{0.96 \pm 0.25}$. We confirm this roughly linear correlation directly by calculating the T_2 required for frms = 10%, using the individual fitted amplitudes (see Fig. 2). In some ways the quantity T_2 is the most obviously physically meaningful, so it seems reassuring that our final conclusion is that this seems to be exactly proportional to luminosity, but that we arrived at this conclusion through fitting two parameters significantly different from unity. More generally the onus is now on theoretical modellers to *predict* values of α and β .

5. DISCUSSION

An appealing possibility is that variability differs from one object to another by having different amounts of the same thing, as for example in shot-noise models, where variability is made up of overlapping flares of some kind. Mathematically, one can always duplicate any power spectrum with such a model, but the simplest and most physically appealing versions are in fact strongly ruled out. Most natural processes are expected to give exponentially decaying flares, for which we expect to see a power spectrum with $\alpha = 2$ at frequencies above

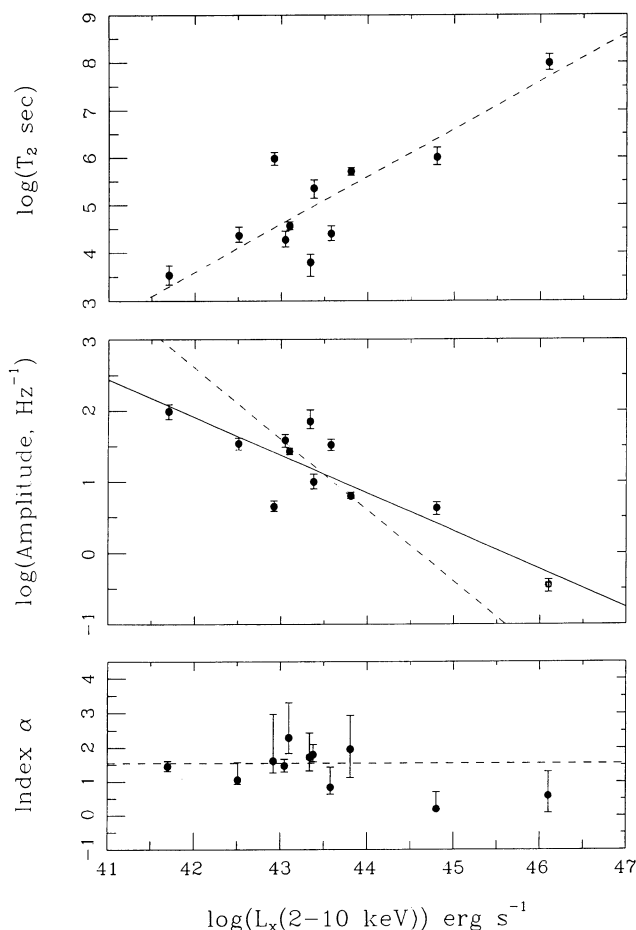


FIG. 2.—Power spectrum fits to *EXOSAT* AGN data. Correlations with $\log(L_x)$, the log of 2–10 keV X-ray luminosity, in ergs s^{-1} , assuming $H_0 = 50 \text{ km s}^{-1} \text{ Mpc}^{-1}$. Error bars throughout are 68% confidence. *Lower frame*: Fitted power spectrum index, α . The dotted line indicates the weighted mean value $\bar{\alpha} = 1.55$. *Middle frame*: Log of the fitted power spectrum amplitude, A . The solid line is the best fit regression, with slope 0.53. The dotted line is a line of slope 1 for illustration. *Upper frame*: Log of the derived value of T_2 , the time scale above which the integrated frms should be 10%. (Time scales for other values of frms will scale as $\text{frms}^{2/(\alpha-1)}$ with $\alpha = 1.55$.) The dotted line is a line of slope 1 for illustration.

the decay time scale, and white noise below this. One can fudge the right α by having shots with a range of decay time scales with a suitable power-law distribution (e.g., Lehto 1989), but it does not seem worth taking this further yet in the absence of a specific physical suggestion. Alternatively one can abandon exponential shots; a shot shape $L(t) \propto t^{-0.23 \pm 0.05}$ would fit the canonical power spectrum. However we can rule out *any* model with shots whose size and shape are fixed, where objects only differ in the number of shots per unit time, λ . This is because $L_x \propto \lambda$ and also $A \propto \lambda/L_x^2$ and so $A \propto L_x^{-1}$, inconsistent with the observed relation $A \propto L_x^{-1/2}$. A successful shot-noise model would require that both λ and the typical shot size scale as $L_x^{1/2}$.

An alternative class of multiple unit models involves a large number of hot spots on a rotating disk, with modulation perhaps by Doppler beaming or by periodic occultation (Abramowicz et al. 1991; Abramowicz 1992). The predicted power spectrum depends on how spot size, lifetime, and surface density vary with radius; but in fact the simplest model, with identical, uniformly distributed, long-lived spots on a Keplerian disk, predicts $\alpha = 5/3$, impressively close to the observed value of $\alpha = 1.55 \pm 0.09$. A further attraction of this class of model is that the amplitude of variations depends strongly on disk inclination, which could explain the scatter in the amplitude versus L_x correlation. However, a specific physical model is needed before taking the rotating hot spot idea more seriously.

The apparently simple scaling of time scale with luminosity suggests that global variations are also a strong possibility (possibly even chaotic variations on a strange attractor—see Lehto, Czerny, & McHardy 1993). For example, hard photons may be created at the center of the source in uncorrelated bursts, and Compton-scatter through the surrounding plasma,

producing filtered white noise. The filter corresponds to the distribution of escape times from the plasma. For a uniform spherical region of modest optical depth, the filter is roughly exponential (Sunyaev & Titarchuk 1980) which implies a power spectrum with $\alpha = 2$. Presumably a combination of the right radial density distribution and optical depth could give the correct power spectrum. Done & Fabian (1989) performed related simulations but added pair production and annihilation through the plasma region; the importance of this is characterized by the “compactness parameter” l . For $l < 1$, they found indeed that $\alpha = 2$; for heavily pair dominated sources, with $l \sim 1000$, they found $\alpha = 1$. Presumably some intermediate compactness will give a good fit to power spectra of AGNs; however, this parameter, as well as the radial density profile, will also determine the output energy spectrum of emerging X-rays. Interestingly, Zdziarski et al. (1990) find that $l \sim 30$ –300 is required to get the right X-ray energy spectrum in such models. The challenge for models is now to find a *consistent* explanation of both the energy spectrum and the power spectrum of variability.

6. CONCLUDING REMARKS

In principle, time series analysis could tell us as much about AGNs as spectral analysis. Now that we have reliable model fits to high-quality light curves, this hope is at last beginning to be realized. Any serious explanation of X-rays from AGNs must explain the typical power spectrum slope of ~ 1.5 , and the fact that the normalized spectral amplitude scales inversely with the square root of luminosity. Some models, such as any with exponential flares, or any where flares are the same in all sources, are already clearly excluded. Hopeful contenders are rotating hot-spot models, and photon diffusion models, but they both need fleshing out.

REFERENCES

- Abramowicz, M. A. 1992, in *Testing the AGN Paradigm*, ed. S. Holt, S. G. Neff, & C. M. Urry (American Institute of Physics Conf. Proc. 254) (New York: AIP), 69
- Abramowicz, M. A., Bao, G., Lanza, A., & Zhang, X.-H. 1991, *A&A*, 245, 454
- Barr, P., & Mushotzky, R. F. 1986, *Nature*, 320, 421
- Belloni, T., & Hasinger, G. 1990a, *A&A*, 227, L33
- . 1990b, *A&A*, 230, 103
- Done, C., et al. 1992, *ApJ*, 400, 138
- Done, C., & Fabian, A. C. 1989, *MNRAS*, 240, 81
- Fiore, F., Massaro, E., & Barone, P. 1992, *A&A*, 261, 405
- Isobe, T., Feigelson, E. D., Akritas, M. G., & Babu, G. J. 1990, *ApJ*, 364, 104
- Lawrence, A., Watson, M. G., Pounds, K. A., & Elvis, M. 1987, *Nature*, 325, 694
- Lehto, H. 1989, in *Two Topics in X-Ray Astronomy*, ed. J. Hunt & B. Batrick (Proc. of 23rd ESLAB Symp.), 499
- Lehto, H., Czerny, B., & McHardy, I. M. 1993, *MNRAS*, 261, 125
- McHardy, I. M. 1988, *Mem. Soc. Astron. Ital.*, 59, 239
- . 1989, in *Two Topics in X-Ray Astronomy*, ed. J. Hunt & B. Batrick (Proc. of 23rd ESLAB Symp.), 1111
- McHardy, I. M., & Czerny, B. 1987, *Nature*, 325, 696
- Mittaz, J. P. D., & Branduardi-Raymont, G. 1989, *MNRAS*, 238, 1029
- Miyamoto, S., Kimura, K., & Kitamoto, S. 1991, *ApJ*, 383, 784
- Papadakis, I. E. 1993, Ph.D. thesis, Univ. of London
- Papadakis, I. E., & Lawrence, A. 1993a, *Nature*, 361, 250
- . 1993b, *MNRAS*, 261, 612
- Stephen, J. B., Bassani, L., Caroli, E., & diCocco, G. 1987, *Nature*, 328, 784
- Sunyaev, R. A., & Titarchuk, L. G. 1980, *A&A*, 86, 121
- van der Klis, M. 1988, in *Timing Neutron Stars*, ed. H. Ogelman & E. P. J. van den Heuvel (Dordrecht: Kluwer), 27
- Zdziarski, A. A., et al. 1990, *ApJ*, 363, L1